SUPPLEMENTAL MATERIAL – ADDITIONAL RESULTS, DISCUSSION AND METHODS

Deformation of Glass-Adsorbed GUVs. Spherical vesicles deform when they adsorb to a glass surface due to the energetically favorable interactions between the surface and the lipid bilayer (1). The precision of the geometrical shape determination of a deformed GUV by epifluorescence microscopy is relatively poor due to the low spatial resolution (especially in the axial direction) relative to the vesicle radius (the lateral and axial resolutions for TR are ~265 nm and ~450 nm, respectively (2)). Nonetheless, a rough estimate of the degree of deformation was obtained. The surface interaction area before GUV rupture (S_v) was estimated from the circular fluorescence intensity pattern observed in the glass surface focal plane. The planar bilayer patch area (S_p) observed after rupture was similarly estimated. S_v/S_p values were independent of GUV size and were between 0.2 and 0.5 for GUVs labeled with 0.5 or 3 mol % TR-DHPE (Fig. S1A). S_v/S_p values are expected to range from 0 to 0.5, since vesicles can adsorb at most half of their total membrane area to the surface (e.g., $S_v/S_p = 0.5$ for a fully flattened, 'pancaked' vesicle). The fact that the S_v/S_p values did not exceed ~0.5 is consistent with the notion that intact vesicles were responsible for the fluorescence patterns observed before the sudden geometrical changes, which occurred within a ~10-20 ms time frame (Fig. 2A), and that planar bilayer patches were responsible for the fluorescence patterns observed after these geometrical changes. Thus, these S_v/S_p data support the hypothesis that these rapid geometrical changes were vesicle rupture events. Further, these data indicate that the adsorbed GUVs were partially flattened. The true extent of the observed deformations is unclear (i.e., it was impossible to distinguish between a quasi-spherical and spherical cap structure) since most S_v values are likely an overestimate of the true adsorbed area due to the poor axial resolution, which prevented distinguishing an adsorbed bilayer from one that was merely close to the surface. Nonetheless, the variable deformations can be approximated by the range of S_v/S_p values (~0.2-0.5) yielding adsorbed vesicle heights from ~0-1.5R (where R is the original GUV radius) (Fig. S1B).

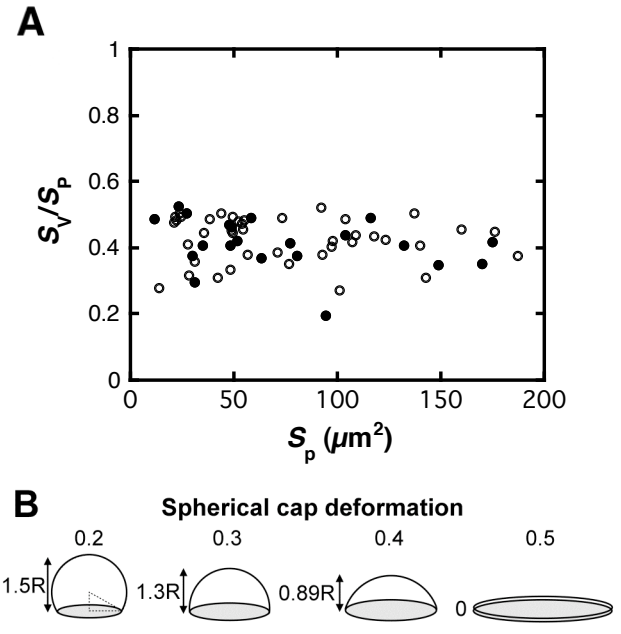

Figure S1. Deformation of Glass-Adsorbed GUVs. (A) S_v/S_p values for DOPC/DOPG (9:1) GUVs labeled with 0.5 mol % TR-DHPE (open circles, $N = 41$) and 3 mol % TR-DHPE (filled circles, $N = 21$). (B) Schematic illustration of vesicle deformation approximated by spherical dome structures with identical surface areas. Geometric shapes are shown for S_v/S_p values of 0.2, 0.3, 0.4, and 0.5. The shadowed regions identify the surface contact areas.

Fluorescence Quenching of NBD-cap PE by Anti-DNP Antibodies in Planar Bilayer Patches. As discussed in the main text, three distinct possibilities exist for the distribution of lipids in a planar bilayer patch relative to the original adsorbed vesicle: the adsorbed bilayer leaflet could arise from the outer vesicle leaflet, the inner vesicle leaflet, or a mixture of the two leaflets. To address this issue of lipid distribution in the planar bilayer patch relative to that in the original vesicle, we took advantage of the fact that anti-dinitrophenol (anti-DNP) antibodies can

quench NBD fluorescence by up to ~96% (3). Considering that the anti-DNP antibody (~152 kDa) is ~7 nm in diameter based on a typical density value for globular proteins (1.35 g/cm^2) (4), we considered it unlikely that the antibody could penetrate into the 1-2 nm thick water layer between the glass surface and the planar bilayer patch (5-7). Therefore, our expectation was that that the antibody would not bind to NBD dyes attached to the lower leaflet of planar bilayers. Further, the NBD dye molecules exposed to the external aqueous solution in vesicles can be selectively reduced with dithionite (8). Thus, we anticipated that selective reduction of outer leaflet NBD dyes coupled with NBD fluorescence quenching after planar bilayer formation would allow us to distinguish among the three lipid redistribution possibilities discussed above (Fig. S2A).

As a first step towards addressing the destination of the lipids in the two GUV leaflets, planar bilayer patches were formed from DOPC/DOPG (9:1) GUVs labeled with 1 mol % NBD-cap PE. After unbound lipids were washed out with a copious amount of buffer, the NBD fluorescence intensities from planar bilayer patches were measured. The samples were then washed with 0.5 μM anti-DNP antibody, and the fluorescence was remeasured ~30 min later. Since both lipid leaflets were tagged with NBD-cap PE in these experiments, all three of the above lipid redistribution possibilities could potentially yield the same result. That is, only about half of the NBD fluorescence would be quenched by anti-DNP antibodies since these antibodies would only bind to those NBD-cap PE lipids in the leaflet exposed to the bulk solution. However, ~95% of the NBD fluorescence was quenched (Fig. S2B). We considered two possible explanations for these data. First, perhaps the anti-DNP antibody had access to the NBD moiety of the NBD-cap PE lipids in the leaflet adsorbed to the glass surface, contrary to our original expectations. This was considered an unlikely possibility due to the large size of the antibody and the small space between bilayer and surface. And second, perhaps the NBD-cap PE lipids in the leaflet adsorbed to the glass surface could migrate to the leaflet exposed to the bulk solution, and once there, anti-DNP antibodies could bind to them and trap them in the upper leaflet. This lipid migration could occur by flip-flop or simple diffusion around the bilayer edge. We define flip-flop here as the transfer of a lipid molecule from one bilayer leaflet to the other through a process that involves passage of the lipid head group through the hydrophobic lipid tail region of the bilayer.

To decipher which of the above interpretations most likely explained the almost complete fluorescence quenching of NBD-cap PE by anti-DNP antibodies in planar bilayer patches, we first examined whether the NBD-cap PE lipid could flip-flop across a bilayer. The external leaflet NBD-cap PE lipids (1 mol %) in DOPC/DOPG (9:1) GUVs were selectively reduced by 20 mM dithionite. After 10-fold dilution (to a concentration of dithionite insufficient to reduce NBD-cap PE) and a 30 min incubation period, the outer leaflet was again exposed to 20 mM sodium dithionite (see Supplementary Material Methods). The expectation was that if significant flip-flop of NBD-cap PE lipids occurs within 30 min, the second dithionite treatment would result in additional reduction of NBD, and hence the bilayers exposed twice to dithionite would exhibit lower NBD fluorescence than the bilayers exposed only once to dithionite. Since fluorescence intensity measurements from planar bilayers entirely within the focal plane are more accurate than those obtained from large spherical vesicles, NBD fluorescence intensities were obtained from planar bilayer patches formed on glass from the GUVs after dithionite treatment. The NBD fluorescence intensities after single and double dithionite treatments were 49 ± 2% (N = 74) and 48 ± 1% (N = 80), respectively, of the intensity obtained for bilayers obtained from unreduced GUVs. Thus, the second dithionite treatment did not significantly reduce the NBD fluorescence intensity from the fluorescence level observed as a result of the first dithionite treatment. Further, the observed fluorescence level was consistent with the hypothesis that complete reduction of the NBD-cap PE in the outer leaflet was accomplished by

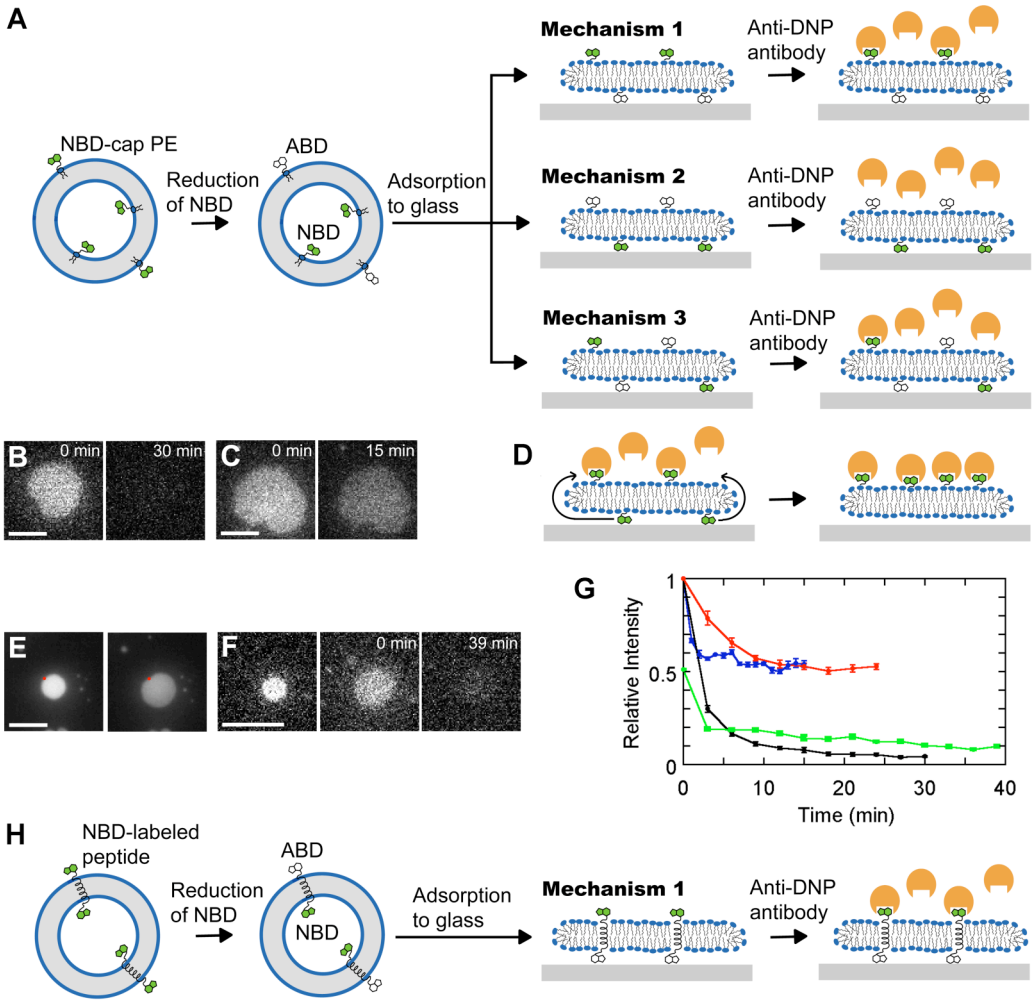

Figure S2. Origin of the Lipids in the Two Bilayer Leaflets of Planar Bilayer Patches. For all images, the focal plane was the glass surface, the bar = 5 μm, and the integration times were 64 ms, unless otherwise noted. (A) Schematic illustrations of the three possible mechanisms whereby the lipids in planar bilayer patches can originate from the two bilayer leaflets of a vesicle, and an approach to determine which possibility is correct. The NBD moieties (*green*) of the NBD-cap PE lipids associated with a vesicle's outer membrane leaflet can be selectively reduced with dithionite to ABD (*colorless*). In planar bilayer patches, anti-DNP antibody (*orange*) can access and quench only those NBD domains associated with the leaflet facing the bulk solution. Thus, if the inner leaflet of the vesicle becomes the leaflet facing the bulk solution after rupture, virtually all of the remaining NBD moieties should be accessible to the anti-DNP antibody after rupture (mechanism 1; after anti-DNP antibody addition, the fluorescence intensity is expected to drop to only a few percent of the original bilayer patch fluorescence intensity). If the outer leaflet of the vesicle becomes the leaflet facing the bulk solution after rupture, virtually none of the remaining NBD moieties should be accessible to the anti-DNP antibody after rupture (mechanism 2; after anti-DNP antibody addition, the fluorescence intensity is expected to remain nearly unchanged). If the lipids in the two vesicle leaflets become completely or partially scrambled before, during, or after rupture, some of the remaining NBD moieties should be accessible to the anti-DNP antibody after rupture (mechanism 3; after anti-DNP antibody addition, the fluorescence intensity is expected to be between 0 and 100% of the original bilayer patch fluorescence intensity). It is not known whether the anti-DNP antibody binds to ABD (assumed here not to bind); however, since ABD is non-fluorescent, the observed fluorescence signal does not depend on this binding interaction. (B) Fluorescence quenching of a DOPC/DOPG (9:1) planar bilayer patch containing 1 mol % NBD-cap PE by the anti-DNP antibody. The original GUV was not treated with dithionite. The NBD fluorescence intensity of the planar bilayer patch was observed at 0 min (*left*). The bilayer was then

(Figure S2 caption continued) washed with 0.5 μM antibody at 0.5 min, and the NBD fluorescence intensity was again observed at 30 min (*right*). Control experiments revealed that no photobleaching was observed for an identical sample that was not treated with antibody. Thus, the ~95% decrease in NBD fluorescence intensity was due solely to quenching by the antibody. (C) Fluorescence quenching of a DOPC/DOPG (9:1) planar bilayer patch containing 1 mol % NBD_2-peptide by the anti-DNP antibody. The original GUV was not treated with dithionite. The NBD fluorescence intensity of the planar bilayer patch was observed at 0 min (*left*). The bilayer was then washed with 2 μM antibody at 0.5 min. The NBD fluorescence intensity decreased to ~53% of the initial value ~14.5 min after antibody addition (*right*). (D) An explanation for the ~95% fluorescence quenching by anti-DNP antibody of NBD-cap PE in planar bilayer patches. The two bilayer leaflets are connected by the high curvature region at the bilayer edge. Thus, the leaflets are no longer independent, and lipids can readily diffuse from one to the other. When an NBD moiety (*green*) on an NBD-cap PE lipid binds to an anti-DNP antibody molecule (*orange*), the lipid can no longer diffuse into the bottom leaflet due to the bulky antibody, which cannot fit into the narrow aqueous layer between the lower leaflet and the surface. Thus, all the NBD-cap PE lipids become trapped in the top leaflet. (E) Rupture of a DOPC/DOPG (9:1) GUV containing 1 mol % NBD_2-peptide. The adsorbed vesicle (*left*) ruptured and formed a planar bilayer patch (*right*) by the asymmetric pathway. Integration time: 12.8 s. (F) Vesicle rupture and NBD fluorescence quenching by anti-DNP antibody for a planar bilayer formed from a DOPC/DOPG (9:1) GUV containing 1 mol % NBD_2-peptide reduced with dithionite (200 mM for 20 min). NBD fluorescence intensities were measured for an adsorbed GUV (*left*) that ruptured to form a planar bilayer patch (*middle*, 0 min). The bilayer patch was washed with 2 μM anti-DNP antibody at 0.5 min, leading to a decrease in the NBD fluorescence intensity by ~82% within 38.5 min (*right*). (G) Time dependence of relative average NBD fluorescence intensities per unit area for various planar bilayer patches treated with anti-DNP antibody. Planar bilayers were prepared as described in (B) (*black*), (C) (*red* and *blue*), and (F) (*green*). Antibody concentrations were 0.5 μM (*black* and *red*) or 2 μM (*blue* and *green*), and were added at 0.5 min. Quenching rate was dependent on antibody concentration, but quenching efficiency was not (compare *red* and *blue*). Except for the green data, initial intensities (0 min; no antibody) were normalized to 1.0. For the green data, the initial intensity was set to 0.51, since this reflects the initial intensity for these dithionite treated samples relative to control samples, which did not undergo dithionite treatment. Shown are the average from multiple bilayer patches: (*black*) $N = 8$; (*red* and *blue*) $N = 11$; (*green*) $N = 4$. Bars show standard errors. (H) Rupture mechanism consistent with the NBD fluorescence quenching data for GUVs labeled with the NBD/ABD-peptide. See text for details. Key same as in (A).

the first dithionite treatment. These data indicate that no significant flip-flop of NBD-cap PE occurs in intact GUVs within 30 min. While it is feasible that the NBD-cap PE flip-flop rate is significantly faster in glass-adsorbed planar bilayers, we consider this unlikely.

Fluorescence Quenching of an NBD-labeled Transmembrane Peptide by Anti-DNP Antibodies in Planar Bilayer Patches. To prevent transfer of an NBD tag from one leaflet to the other by diffusion around a bilayer patch edge, we designed a peptide that spanned both lipid leaflets. The amino acid sequence of the peptide, $KR_2L_{19}R_2K$, was expected to span a bilayer membrane once in a helical configuration. The hydrophobic stretch of leucines was expected to anchor the peptide in the hydrophobic core of the bilayer lipid while the hydrophilic, charged, arginines near the N- and C-termini were expected to prevent reorientation (flip-flop) of the transmembrane peptide within the bilayer. The two lysines at the N- and C-termini were labeled with NBD (forming NBD_2-peptide) before use (see Supplementary Material Methods). Unlike NBD-cap PE, which spans only a single membrane leaflet and thus could potentially diffuse around the edge of a bilayer into the other leaflet, we anticipated that the bilayer spanning peptide would not be able to reorient within the membrane at a bilayer edge.

Having constructed the above fluorescent peptide, we tested whether it behaved as designed. Bilayer patches were formed from GUVs that contained 1 mol % NBD_2-peptide. At 2 μM anti-DNP antibody, the fluorescence of the bilayer patches was reduced to ~53% of the initial value in ~15 min (Fig. S2C). These data indicate that only about half of the NBD dyes attached to the peptide were accessible to the anti-DNP antibody. Since the peptide was designed such that for each NBD_2-peptide molecule one NBD molecule would be positioned near the aqueous interface of each bilayer leaflet, these data support the picture that the NBD dyes of one of the two leaflets was inaccessible to the antibody. Further, since it is more reasonable that the NBD dyes

associated with the leaflet facing the bulk solution were more accessible to the anti-DNP antibody than those NBD dyes associated with the leaflet facing the glass surface, our original assumption that the anti-DNP antibody could not access NBD dyes between the glass surface and the adsorbed leaflet was considered correct. Thus, we conclude that the most likely explanation as to why ~95% of the fluorescence of NBD-cap PE lipids was quenched by the anti-DNP antibody (Fig. S2B) is that the NBD-cap PE lipids migrated to the leaflet exposed to the bulk solution, not by flip-flop, but by diffusing through a highly curved lipid structure at the bilayer edge (Fig. S2D).

To test whether the NBD_2-peptide altered the GUV rupture mechanism, we examined the fluorescence patterns of adsorbed vesicles and the resultant planar bilayer patches for GUVs containing NBD_2-peptide. By comparing the fluorescence patterns observed with those observed earlier for GUVs labeled with TR-DHPE (Fig. 2), we concluded that GUVs containing NBD_2-peptide formed planar bilayers via the asymmetric rupture pathway (Fig. S2E) for all vesicles examined ($N = 9$). Therefore, the NBD_2-peptide did not appear to significantly alter the rupture mechanism.

Next, we tested whether the NBD associated with the outer leaflet in GUVs containing NBD_2-peptide could be selectively reduced by dithionite. The GUVs were reacted with 100, 200, and 300 mM dithionite for 20 min. Higher dithionite concentrations were required to reduce the NBD attached to the peptide than to reduce the NBD moiety of NBD-cap PE. As discussed above for the dithionite reduction of NBD-cap PE, the NBD fluorescence intensity was measured after GUVs had ruptured on a glass surface and unbound lipids were removed by extensive washing. Compared with the fluorescence intensities of bilayer patches obtained from GUVs containing NBD_2-peptide that had not been treated with dithionite, the NBD fluorescence intensities of the bilayer patches formed from the GUVs containing NBD_2-peptide reacted with 100, 200, and 300 mM dithionite were 50±3%, 51±4%, and 48±3% (N = 36-43), respectively. These data are consistent with the hypothesis that dithionite completely reduced the NBD moieties associated with the outer leaflet.

The anti-DNP antibody was then used to determine the accessibility of the remaining fluorescent NBD molecules in bilayer patches formed from dithionite-treated (200 mM) GUVs containing NBD_2-peptide. GUVs ruptured via the asymmetric pathway, suggesting that the dithionite reduced peptide did not affect the rupture process. The NBD fluorescence intensity from bilayer patches was quenched ~82% by 2 μM anti-DNP antibody (Figs. S2F and S2G). According to the above control experiments, dithionite treatment selectively reduces the NBD moieties associated with the outer bilayer leaflet of intact vesicles, and the fluorescence intensity from the NBD moieties that remain after dithionite treatment can only be quenched if they are associated with the bilayer leaflet exposed to the bulk solution. These antibody quenching data therefore support the hypothesis that when a GUV ruptures, it is primarily the outer leaflet of the GUV that becomes the bilayer leaflet adsorbed to the glass surface in the resultant bilayer patch (Fig. S2H).

Energetics of Isolated GUV Rupture. The conversion of a GUV into an adsorbed planar bilayer patch requires formation of a bilayer edge, which surrounds the patch. Bilayers edges are energetically unfavorable, unless positive curvature lipids are present to partition into the high curvature edge structure. Since adsorbed bilayer patches from single GUVs are stable once formed (they remained stable for the longest time we examined them, ~2 hrs, with no sign of decomposition), we calculated the rupture energetics (Fig. S3; details in Supplementary Material Methods). We first estimated the free energy change for conversion of a DOPC or DOPE-Me GUV into a planar bilayer disk in solution (ΔG_{sol}). As expected, ΔG_{sol} is positive due to the

unfavorable edge energy. The change in curvature energy ($G_{curv,v} - G_{curv,p}$) is small compared to the line tension (edge energy), and thus the ΔG_{sol} is approximately linearly dependent on the GUV radius (edge length equivalent to the circumference, which in turn is proportional to the radius) (Figs. S3B and S3C). The free energy for conversion of a GUV into a glass adsorbed planar bilayer disk (ΔG_{surf}) is equivalent to the ΔG_{sol} plus the adsorption free energy, i.e., $\Delta G_{surf} = \Delta G_{sol} + G_{ads}$. Since the interaction of a bilayer with glass is favorable, G_{ads} is negative for all patch sizes. For large vesicle radii, the magnitude of G_{ads} is much larger than that of ΔG_{sol}, and thus ΔG_{surf} is large and negative (Figs. S3B and S3C), indicating that adsorbed planar bilayer formation is highly favorable under these conditions. However, the magnitude of the adsorption energy depends on the square of the radius. For small radii (< ~0.6 μm), G_{ads} is insufficient to compensate for ΔG_{sol}, and ΔG_{surf} is positive (Fig. S3D). Thus, these calculations predict that the isolated rupture of DOPC vesicles with radii < ~0.6 μm is energetically unfavorable. The rupture of DOPE-Me vesicles is more unfavorable than the rupture of DOPC vesicles for small radii, but more favorable for large radii (Fig. S3D). These calculations indicate that the rupture of GUVs with both low and high $C_{0,ave}$ values is energetically favorable. Though one possibility is that low $C_{0,ave}$ GUVs do not undergo isolated rupture (Fig. 5) for kinetic reasons, it is also reasonable that the greater energetic instability of rupture pores in low $C_{0,ave}$ vesicles inhibits the formation of a rupture pore sufficiently large to catalyze vesicle rupture.

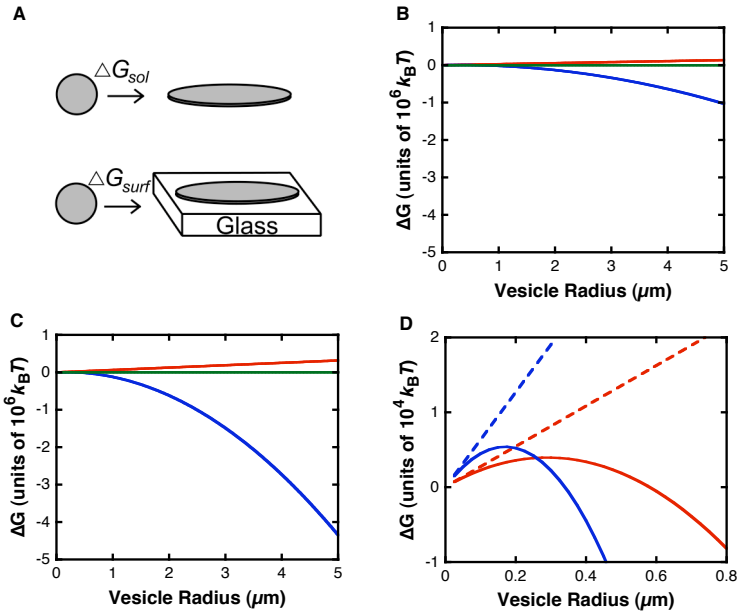

Figure S3. Energetics of Vesicle Rupture on Glass. Vesicle rupture energetics calculated as described in Methods. (A) Reactions described by ΔG_{sol} and ΔG_{surf}. For (B) DOPC vesicles and (C) DOPE-Me vesicles: (*red*) ΔG_{sol}; (*green*) $G_{curv,v} - G_{curv,p}$; (*blue*) ΔG_{surf}. (D) Expanded scale for both DOPC (*red*) and DOPE-Me (*blue*) vesicles: (*dashed*) ΔG_{sol}; (*solid*) ΔG_{surf}.

METHODS

Dye-Labeling of the $KR_2L_{19}R_2K$ Peptide. An established method (9) guided the purification of the $KR_2L_{19}R_2K$ peptide. The impure peptide (as received from the manufacturer) was solubilized in water/isopropanol/trifluoroacetic acid (TFA) (50:50:0.1) (v/v/v) at ~2 mg/mL and loaded onto a C2/C18 reverse-phase column (GE Healthcare, Piscataway, NJ) equilibrated with the same buffer. The chromatography system was maintained at 4°C. The peptide was eluted by linearly increasing the isopropanol concentration from 50 to 90% (5% per column volume) at 0.1 mL/min. The dominant peak (absorbance at 225 nm) observed at ~64% isopropanol was analyzed by MALDI mass spectrometry. The observed major monocationic $(M+H)^+$ peak at m/z = 3090.33 is consistent with the expected value for the unprotonated peptide (MW = 3089.23 g/mol). Thus, we concluded that the species eluting at ~64% isopropanol was purified peptide.

Having established that the impure peptide mixture obtained from the manufacturer contained the desired peptide, the terminal lysines were labeled with NBD. Our expectation was that the two terminal lysines would react with NBD succinimide, yielding a peptide tagged at each end with an NBD dye. The impure peptide was solubilized at ~2 mg/mL in DMSO containing 400 mM triethanolamine, and then was mixed with 10 mg/mL NBD succinimide in DMSO to yield a final peptide:dye molar ratio of 1:10. After overnight incubation at room temperature in the dark, isopropanol was added to the reaction mixture (to ~30 vol %) to prevent freezing the DMSO solvent in the chromatography column maintained at 4°C. The dye-labeled peptide was purified using the procedure described above for the unlabeled sample, except that the eluate absorption was monitored at both 225 and 466 nm. No peak was observed at ~64% isopropanol, and no peaks were observed that yielded an absorbance at 225 nm without a concommittant absorbance at 466 nm. Thus, within experimental error, no unlabeled peptide remained in the reaction mixture. The dominant peak (absorbance at 446 nm) observed at ~71% isopropanol was analyzed by mass spectrometry. LC/MS MS yielded a collision induced dissociation pattern consistent with that expected for the NBD-labeled peptide (NBD_2-peptide). Aromatic NBD groups were expected to make the peptide more hydrophobic. The elution of the NBD-labeled peptide at a higher isopropanol concentration (~71%) than the unlabeled peptide (~64%) was consistent with this expectation. The fractions containing chromatographically purified NBD_2-peptide were pooled, and chloroform was added to extract the peptide into an organic phase. After removal of the water phase, the solvent of the organic phase was evaporated under a stream of nitrogen, and the residue was then dried under house vacuum for 8 h. The NBD_2-peptide was dissolved in isopropanol to yield a concentration of 0.1 mM, as determined by the absorption at 466 nm. Peptide stock solutions were stored at -20°C.

NBD Reduction and Flip-Flop Assay for DOPC/DOPG (9:1) GUVs labeled with 1% NBD-cap PE. Sodium dithionite was used to selectively render non-fluorescent the outer membrane leaflet of intact NBD-containing vesicles. The dithionite anion ($S_2O_4^{2-}$) does not penetrate bilayer membranes. Thus, when vesicles containing NBD-labeled phospholipids were incubated with dithionite, only the NBD dyes located on the outer leaflet were reduced. $S_2O_4^{2-}$ is in equilibrium with SO_2^- radical, the species that reduces NBD to 7-amino-2,1,3-benzoxadiazol-4-yl (ABD). ABD-labeled lipids do not show significant fluorescence when illuminated with 470 nm light, a wavelength that produces significant NBD fluorescence (8).

For NBD reduction, 1 M sodium dithionite stock solutions were freshly prepared in 1 M Tris-HCl, pH 10.0 before use. Sodium dithionite is highly susceptible to spontaneous breakdown (8), making aqueous solutions acidic as it is oxidized to SO_3^{2-} and SO_4^{2-} in the presence of aqueous dioxygen. Thus, the high buffer concentration was used to inhibit acidification. GUVs containing 1 mol % NBD-cap PE (0.8 mg/mL total lipids) were incubated with 20 mM dithionite in 200 mM HEPES, pH 8.0 for 5 min. The NBD reduction reaction was stopped by 10-fold dilution with Buffer A. To determine whether NBD-cap PE could translocate from one leaflet to the other (i.e., flip-flop), the reduced samples were incubated at room temperature for 30 min to allow for lipid flip-flop. The dithionite concentration was again brought to 20 mM (lipid concentration 0.08 mg/mL) for 5 min. The sample was then diluted 10-fold with Buffer A to stop NBD reduction.

Reduction of DOPC/DOPG (9:1) GUVs labeled with 1% NBD_2-peptide. The NBD_2-peptide was designed to have a hydrophobic central region that could span the membrane bilayer, and to have positive charges at each terminus to prevent flip-flop. GUVs containing 1%

NBD_2-peptide (1.6 mg/mL total lipids) were incubated with 100, 200, or 300 mM dithionite in 200 mM HEPES, pH 8.0 for 20 min. NBD reduction was stopped by 100-fold dilution with Buffer A. The higher dithionite concentrations required to reduce the NBD on the peptide compared with the NBD on the PE lipid precluded the flip-flop assay discussed above, which required two dithionite additions and dilutions (to initiate and halt reduction, respectively).

Fluorescence Microscopy of NBD-cap PE and NBD_2-peptide Labeled Bilayers. When GUVs labeled with NBD-cap PE or NBD_2-peptide were reacted with dithionite, NBD reduction was confirmed after vesicle rupture. GUVs at lipid concentrations of 0.08, 0.04, and 0.004 mg/mL were incubated on the coverslip surface for 3, 20, and 40 min, respectively. After the surface was rinsed with Buffer A to remove unbound lipids, the NBD fluorescence was measured for planar bilayer patches formed from the vesicles.

For NBD fluorescence quenching experiments with anti-DNP antibody, flow chambers (10-20 μL volume) were made with strips of high vacuum grease sandwiched between glass slides. GUVs were added at 0.008 mg/mL lipid in Buffer A. Samples were washed with ~8 chamber volumes of Buffer A. GUVs that were not treated with dithionite were incubated for 15 min to insure vesicle rupture. Dithionite-treated GUVs were incubated until the rupture pathway for a unilamellar vesicle of interest was established; anti-DNP antibody was added shortly thereafter, minimizing the opportunity for membrane leaflets to mix between rupture and antibody treatment. The time-dependent NBD fluorescence quenching with anti-DNP antibody was begun immediately after washing with ~3 chamber volumes of the antibody solution. The anti-DNP stock solution (2 mg/mL) was diluted with Buffer A.

Free Energy Calculations. A single-lipid bilayer with total surface area, A, is described by the free energy (10-12):

$$G = \underbrace{\frac{k_c}{2}\oint dA(C_1 + C_2 - C_0)^2 + k_g \oint dA(C_1 C_2)}_{G_{curv}} + \underbrace{\frac{k_c}{2}\oint dA^*(C_1^* + C_2^* - C_0)^2}_{G_{line}} + \underbrace{WA_1}_{G_{ads}} + PV + \Sigma A \qquad (1)$$

In this expression, the first two terms represent the curvature energy, G_{curv}, where k_c and k_g are the bending modulus, and the Gaussian curvature modulus, respectively. The principle curvatures, C_1 and C_2, are equivalent to the inverse of the principle radii, and are equal for a spherical vesicle (13,14). The third term is the energy due to the line tension, G_{line}, where the starred (*) values represent the area and principle curvatures of the bilayer edge region, e.g., resulting from the bilayer edge within a rupture pore or on a surface adsorbed bilayer disk (12). The fourth term is the adsorption energy, G_{ads}, for the area, A_1, in contact with a surface. The fifth term represents the energy due to the osmotic pressure difference, P, for a vesicle of volume, V. The sixth term arises from the lateral tension, Σ. For the free vesicle and adsorbed planar disk situations considered here, the last two terms are small or zero, and therefore, are ignored below.

For a vesicle of radius, R (measured from the spherical center to the center of the bilayer), in solution, the G_{curv} is given by:

$$G_{curv,v} = 2\pi k_c \left[\left(R + 0.5d\right)^2 \left(\frac{2}{R + 0.5d} - C_0\right)^2 + \left(R - 0.5d\right)^2 \left(\frac{-2}{R - 0.5d} - C_0\right)^2 \right] + 8\pi k_g \qquad (2)$$

where the first two terms denote the curvature contributions from the outer and inner leaflets, respectively. For a planar bilayer disk, $C_1 = C_2 = 0$, and hence the G_{curv} is given by:

$$G_{\text{curv,p}} = 4\pi k_c R^2 (C_0)^2 \quad (3)$$

Here it was assumed that a vesicle with radius, R, and surface area, $4\pi R^2$, was converted to a circular, surfaced-adsorbed, planar bilayer disc with radius, $2R$, and surface area, $4\pi R^2$. There is no line tension contribution for an intact vesicle, but a planar bilayer disk (radius $2R$) has an edge area determined by its circumference and bilayer thickness (12), yielding a G_{line} of:

$$G_{\text{line,p}} = 2k_c \pi^2 dR\left(\frac{2}{d} + \frac{1}{2R} - C_0\right)^2 \quad (4)$$

where d is the distance between the pivotal planes of the two lipid monolayers. The pivotal plane is close to the boundary between the hydrocarbon and polar regions of the lipid monolayer (15). The adsorption energy of a planar bilayer disk to a surface, G_{ads}, is proportional to the total area of the disk (radius $2R$):

$$G_{\text{ads,p}} = 4\pi R^2 W \quad (5)$$

Using the above equations, the free energy for conversion of a vesicle to a planar bilayer disk in solution is given by:

$$\Delta G_{\text{sol}} = \left(G_{\text{curv,p}} + G_{\text{line,p}}\right) - \left(G_{\text{curv,v}}\right) \quad (6)$$

Since $G_{\text{line,p}} >> (G_{\text{curv,p}} - G_{\text{curv,v}})$ and ΔG_{sol} is positive, a vesicle is stable to rupture primarily due to the unfavorable line energy. For conversion of an intact vesicle to a surface adsorbed planar bilayer disk, the free energy is given by:

$$\Delta G_{\text{surf}} = \left(G_{\text{curv,p}} + G_{\text{line,p}} + G_{\text{ads,p}}\right) - \left(G_{\text{curv,v}}\right) = \Delta G_{\text{sol}} + G_{\text{ads,p}} \quad (7)$$

Since $G_{\text{ads,p}}$ is negative for glass (strong interaction between bilayer and surface), vesicle rupture is energetically favorable if the energetically unfavorable line tension is compensated for by a strong surface interaction.

Our primary purpose for calculating ΔG_{sol} and ΔG_{surf} was to compare the effect of intrinsic curvature on the energetics of vesicle rupture. C_0 values for DOPC and DOPE-Me were given in the main text. A DOPC bilayer has a spacing between pivotal planes (d) of ~2.7 nm (16). The k_c for DOPC is ~7 k_BT; since the k_c for DOPE is ~11 k_BT and DOPC is triply methylated DOPE, we estimate that the k_c for DOPE-Me (singly methylated) is ~10 k_BT (12,17). For DOPC, $k_c \approx$ -0.3 k_g; for DOPE-Me, $k_c \approx$ -0.83 k_g (18,19). The strength of the interaction between DOPC bilayers and glass was estimated as ~0.15 mJ/m^2 (W) (20); the affinity of DOPE-Me bilayers for glass was estimated to be ~4-fold higher ($W \approx$ ~0.60 mJ/m^2), based on the differential affinity of DOPC and DOPE for mica (21).

REFERENCES

1. Seifert, U. 1997. Configurations of fluid membranes and vesicles. *Adv. Phys.* 46:13-137.
2. Murphy, D. B. 2001. Fundamentals of Light Microscopy and Electronic Imaging. A John Wiley and Sons, New York.
3. Lancet, D., and I. Pecht. 1977. Spectroscopic and immunochemical studies with nitrobenzoxadiazolealanine, a fluorescent dinitrophenyl analog. *Biochemistry* 16:5150-5157.
4. Fischer, H., I. Polikarpov, and A. F. Craievich. 2004. Average protein density is a molecular-weight-dependent function. *Prot. Sci.* 13:2825-2828.
5. Koenig, B. W., S. Kruger, W. J. Orts, C. F. Majkrzak, N. F. Berk, J. V. Silverton, and K. Gawrisch. 1996. Neutron reflectivity and atomic force microscopy studies of a lipid bilayer in water adsorbed to the surface of a silicon single crystal. *Langmuir* 12:1343-1350.

6. Johnson, S. J., T. M. Bayerl, D. C. Mcdermott, G. W. Adam, A. R. Rennie, R. K. Thomas, and E. Sackmann. 1991. Structure of an adsorbed dimyristoylphosphatidylcholine bilayer measured with specular reflection of neutrons. *Biophys. J.* 59:289-294.
7. Bayerl, T. M., and M. Bloom. 1990. Physical properties of single phospholipid-bilayers adsorbed to micro glass-beads - a new vesicular model system studied by H-2 nuclear magnetic resonance. *Biophys. J.* 58:357-362.
8. McIntyre, J. C., and R. G. Sleight. 1991. Fluorescence assay for phospholipid membrane asymmetry. *Biochemistry* 30:11819-11827.
9. Lew, S., and E. London. 1997. Simple procedure for reversed-phase high-performance liquid chromatographic purification of long hydrophobic peptides that form transmembrane helices. *Anal. Biochem.* 251:113-116.
10. Lipowsky, R., and U. Seifert. 1991. Adhesion of vesicles and membranes. *Mol. Cryst. Liq. Cryst.* 202:17-25.
11. Gruner, S. M. 1989. Stability of lyotropic phases with curved interfaces. *J. Phys. Chem.* 93:7562-7570.
12. Karatekin, E., O. Sandre, H. Guitouni, N. Borghi, P. H. Puech, and F. Brochard-Wyart. 2003. Cascades of transient pores in giant vesicles: line tension and transport. *Biophys. J.* 84:1734-1749.
13. Lipowsky, R. 1991. The conformation of membranes. *Nature* 349:475-481.
14. Rand, R. P., and V. A. Parsegian. 1997. Hydration, curvature, and bending elasticity of phospholipid monolayers. *In* Lipid Polymorphism and Membrane Properties. Epand RM, editor. Academic Press, San Diego. 375-401.
15. Fuller, N., and R. P. Rand. 2001. The influence of lysolipids on the spontaneous curvature and bending elasticity of phospholipid membranes. *Biophys. J.* 81:243-254.
16. Lee, A. G. 2003. Lipid-protein interactions in biological membranes: a structural perspective. *Biochim. Biophys. Acta* 1612:1-40.
17. Chen, Z., and R. P. Rand. 1997. The influence of cholesterol on phospholipid membrane curvature and bending elasticity. *Biophys. J.* 73:267-276.
18. Kozlovsky, Y., A. Efrat, D. A. Siegel, and M. M. Kozlov. 2004. Stalk phase formation: effects of dehydration and saddle splay modulus. *Biophys. J.* 87:2508-2521.
19. Siegel, D. P., and M. M. Kozlov. 2004. The Gaussian curvature elastic modulus of N-monomethylated dioleoylphosphatidylethanolamine: relevance to membrane fusion and lipid phase behavior. *Biophys. J.* 87:366-374.
20. Schonherr, H., J. M. Johnson, P. Lenz, C. W. Frank, and S. G. Boxer. 2004. Vesicle adsorption and lipid bilayer formation on glass studied by atomic force microscopy. *Langmuir* 20:11600-11606.
21. Marra, J., and J. Israelachvili. 1985. Direct measurements of forces between phosphatidylcholine and phosphatidylethanolamine bilayers in aqueous electrolyte solutions. *Biochemistry* 24:4608-4618.